



## An analytical wall heat flux distribution model for re-entry vehicle pre-design activities

Y. Prevereaud<sup>1</sup>, J.-L. Vérand<sup>2</sup>, S. Galera<sup>3</sup>

### Abstract

The evaluation of the wall heat flux in hypersonic regime is crucial for the design of any space vehicle and mission. To quickly estimate the wall heat flux during vehicle pre-design phase, surrogate models are mandatory. The aim of the present work is to evaluate the strengths and weaknesses of the current models and to develop a general and efficient formulation, i.e. able to quickly obtain accurate results for any object shape. Hence, a numerical database including a large variety of space objects (gliding vehicles, capsules, space debris) has been built and analyzed. A new surrogate model has been then developed and successfully validated by comparison with CFD results.

**Keywords:** *Wall Heat Flux, Surrogate model, Hypersonic vehicle, atmospheric entry*

### Nomenclature

M – Mach number  
P – Pressure  
Q – Wall heat flux  
R – Curvature radius  
s – Curvilinear abscissa  
u – Velocity  
Z – Altitude

$\beta$  – Side slip angle  
 $\theta$  – Wall inclination compared to vehicle  
velocity vector

Subscripts  
e – outside of the boundary layer  
stag – stagnation point  
 $\infty$  – freestream values

$\alpha$  – Angle of attack

### 1. Introduction

The estimation of the wall heat flux in the hypersonic regime is an essential pre-requisite for the design of any space vehicle and mission. To explore a large number of vehicle designs, trajectories and Thermal Protection System (TPS) in the pre-design phase, especially during Concurrent Design Engineering activities, surrogate or analytical models are mandatory. Indeed, although high fidelity physical models are relatively accurate, they cannot characterize, in a short time (few minutes), a whole trajectory or an important number of selected flight points for each given vehicle design. On the other hand, analytical models allow to quickly compute the wall heat flux distribution but with a higher uncertainty level and for limited configurations (flight points or shapes). The objective of the presented work is to evaluate the analytical models currently used and described in open literature by comparison with CFD results from an extensive database. Then, the following step is to develop a general and efficient formulation, i.e. a formulation allowing to quickly obtain results close to the CFD solutions for any object shape.

<sup>1</sup> ONERA, 2 avenue Edouard Belin, 31055 Toulouse, France, [ysolde.prevereaud@onera.fr](mailto:ysolde.prevereaud@onera.fr)

<sup>2</sup> ONERA, 2 avenue Edouard Belin, 31055 Toulouse, France, [jean-luc.verant@onera.fr](mailto:jean-luc.verant@onera.fr)

<sup>3</sup> CNES, 18 avenue Edouard Belin, 31400 Toulouse, France, [stephane.galera@cnes.fr](mailto:stephane.galera@cnes.fr)

## 2. Literature review

A certain number of models allowing to determine the heat flux distribution at the wall of objects of various shapes can be found in literature. Those models generally describe the ratio between the local heat flux and the stagnation point heat flux, and not directly the local heat flux. Moreover, these models were built assuming flow at thermochemical equilibrium in the shock layer. Finally, some models were developed assuming laminar boundary layers, and others for turbulent boundary layers. Since the nature of the boundary layer is modified during the atmospheric reentry (increase of the Reynolds number, wall roughness), having a model for the laminar regime and another for the turbulent regime is necessary to correctly predict the heat flux along the whole entry trajectory.

The well-known Lees model [1], developed in 1956 to predict the laminar heat transfer on axisymmetric blunt bodies in case of hypersonic flow in thermochemical equilibrium, is based on the boundary layer equations and the local similarity assumption:

$$\frac{Q(x,y,z)}{Q_{stag}} = \frac{1}{2} \times \frac{\frac{p}{p_{stag}} \frac{u_e}{u_\infty} r \sqrt{R_{stag}}}{\left( \int_0^s \frac{p}{p_{stag}} \frac{u_e}{u_\infty} r^2 ds \right)^{0.5} \sqrt{\frac{1}{u_\infty} \left( \frac{du_e}{d\theta} \right)_s}} \quad (1)$$

Simplified expressions of Eq. 1 can be obtained for spheres and sphere-cones making additional assumptions.

In 1959, Kemp *et al.* [2] developed a model able to determine the laminar heat flux along an axisymmetric blunt body, without incidence, in a dissociated air flow represented as a mixture of air molecules and atoms. Unlike Lees [1], the local similarity differential equations are solved exactly with the external pressure gradient parameter, the variable  $\rho\mu$  and the inclusion of the dissipation term. Thus, in the solution proposed by Kemp *et al.* [2], the characteristics of the boundary layer evolve around the object, offering the possibility to calculate the non-similar terms in the integral equations and thus to estimate the validity of the local similarity assumption for any particular case. However, the Kemp formulation is difficult to apply. Some authors indicate that, based on the experimental results obtained by Kemp, the heat flux distribution from the stagnation point for a hemispherical cylinder can be approximated by the following formulation (named "Kemp modified" in the following):

$$\frac{Q(x,y,z)}{Q_{stag}} = \cos\left(\frac{\theta}{2}\right)^{5.27} \quad (2)$$

Murzinov [3] proposed in 1966 a model for the estimation of the convective heat flux distribution around a sphere, in the case of a dissociated laminar boundary layer in thermochemical equilibrium:

$$\frac{Q(x,y,z)}{Q_{stag}} = 0.55 + 0.45 \cos(2\theta) \quad (3)$$

These models were developed for specific geometric shapes. However, there are other models in the literature that claim to be generalist such as Vérant-Lefrançois [4] model, Mierrfield model [6] or the model used in the Spacecraft-Oriented code SCARAB [5].

The Vérant-Lefrançois equation (Eq. 4) was confronted with numerical and experimental results on different object shapes. Although good results are generally obtained for convex shaped objects, this formulation is faulty in the case of flat or concave walls:

$$\frac{Q(x,y,z)}{Q_{stag}} = \left( \frac{P(x,y,z)}{P_{stag}} \right)^a \left( \frac{R_{stag}}{R(x,y,z)} \right)^b \quad (4)$$

Results obtained with literature models have been compared to numerical results for different kind of shapes (Fig. 1). The analysis reveals that some models described in the literature allow to obtain correct results for convex blunt objects. The Vérant-Lefrançois model allow to obtain a heat flux close to that determined numerically on a wide variety of shapes. The Murzinov model, although developed for spheres only, offers better results than generalist models. All these models are however faulty in a number of known cases : concave walls, flat walls (Fig. 2), in the presence of specific physical phenomena such as a reduction in the thickness of the boundary layer at the trailing edge (Fig. 3), shock-shock interactions or shock-boundary layer interactions. The development of a more complete and generalist model for the calculation of the parietal heat flux distribution is necessary. For this, an extensive numerical database is then mandatory.

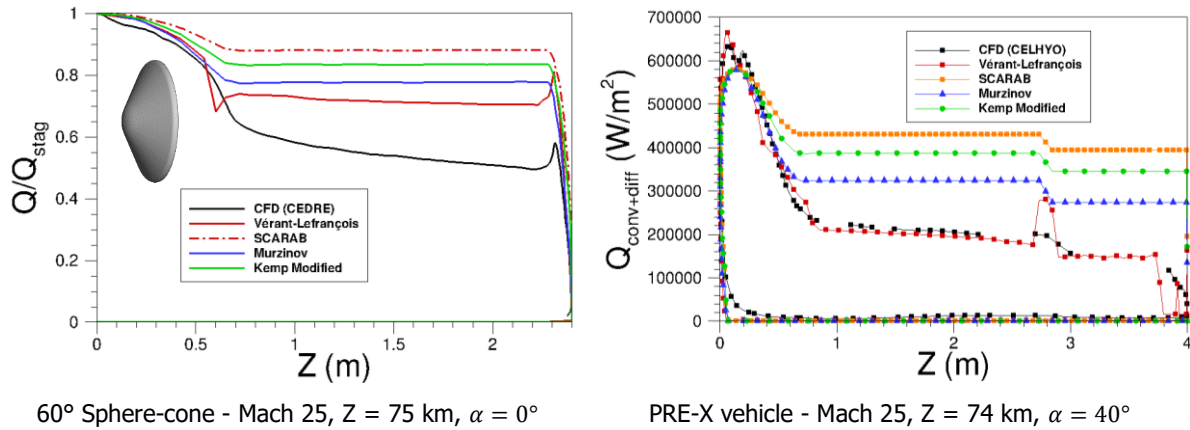


**Fig. 1.** Comparison of wall heat flux distribution obtained with analytical models and CFD simulations for convex objects.

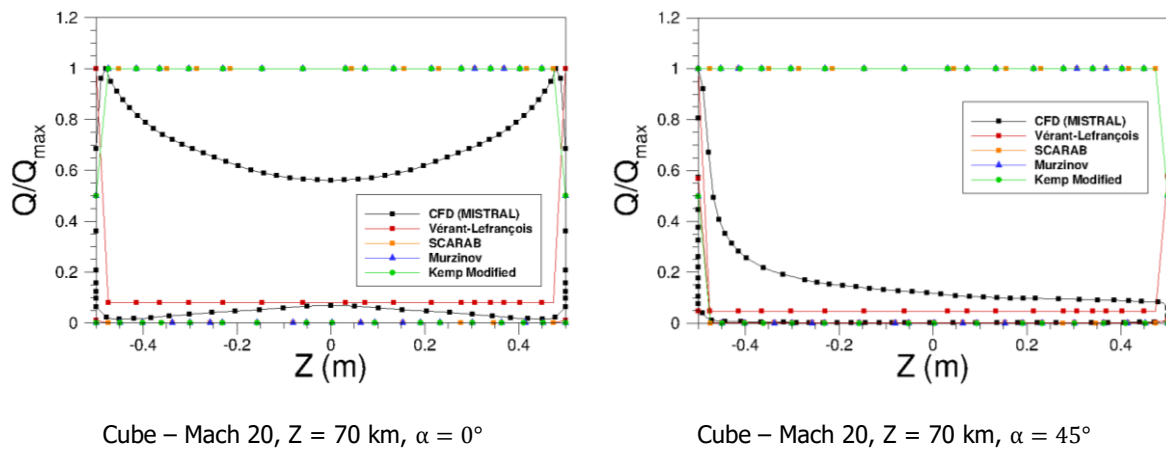


**Fig. 2.** Comparison of wall heat flux distribution obtained with analytical models and CFD simulations for a cube with and without angle of attack  $\alpha$ .

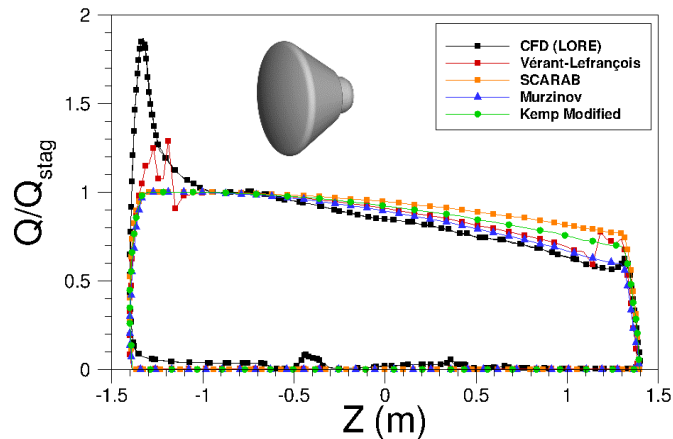


**Fig. 3.** Comparison of wall heat flux distribution obtained with analytical models and CFD simulations for ARD – Mach 24, Z = 65 km,  $\alpha = 20^\circ$ .

### 3. Numerical database

The numerical database is composed of 2D-axisymmetric and 3D Navier-Stokes simulations around a wide variety of shapes (Fig. 4), objects attitude (angle of attack  $\alpha$ , side slip angle  $\beta$ ) and flight points (altitude, velocity). The object size is between 0.05 m and 65 m. According to the considered object,  $\alpha$  and  $\beta$  varies from  $0^\circ$  to  $90^\circ$ . In terms of flight points, a wide range of altitude-Mach number has been considered along characteristic spacecraft and space debris characteristic trajectories:  $30 \text{ km} \leq Z \leq 90 \text{ km}$ ,  $2 \leq M_\infty \leq 35$ .

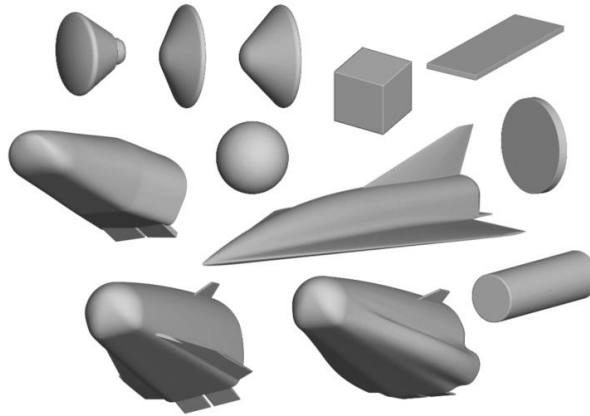


**Fig. 4.** Objects shapes of the numerical database.

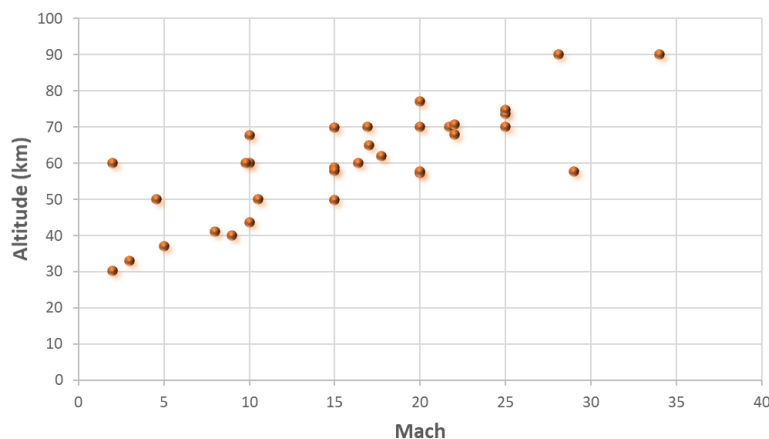


**Fig. 5.** Flight points (altitude as a function of the Mach number) at which the CFD solutions of the database have been calculated.

Different Navier-Stokes codes (CELHYO, CEDRE, LORE, MISTRAL) were used to generate the database.

**CELHYO** [8] is a fluid mechanics code developed at ONERA to simulate reactive continuous hypersonic flows. The 3D Navier-Stokes equations are solved using an implicit GMRES scheme. A set of chemical reactions can be specified accounting for flows in chemical non-equilibrium. The solver uses the HUS scheme (Hybrid Upwind Scheme) for the evaluation of inviscid flows. A second-order precision in space is obtained by using an extrapolation of the MUSCL scheme. In the regions with strong discontinuity (shock), the minmod limiter is used.

**CEDRE** [9] is the multi-physics simulation platform developed by ONERA including a number of solvers like CHARME. CHARME is an unstructured Navier-Stokes solver. The Navier-Stokes equations are discretized by second order finite-volume approach and an AUSM+ flux scheme associated with a Van Leer limiter. Temporal integration is performed with a full implicit approach. No turbulence model is used here. Park's chemical kinetics model with 5 species and 17 reactions is used. However, the state of the gas depends on the flight point, the shape and the attitude of the object under consideration. Also, according to these parameters, locally, the flow can be an ideal gas or a real gas in chemical non-

equilibrium or at equilibrium. In other words, the flow is set free to get into a state that corresponds to the local conditions encountered. Some simulations were carried out with a Park model with 11 species and 51 reactions. Finally, others were carried out with an imposed wall temperature (500 K and 700 K), while the majority of the simulations were carried out by solving the heat balance at the wall, whose emissivity is assumed to be equal to 0.8 (radiative equilibrium temperature).

**LORE** [10] is a multiblock structured code from ESA, covering all flow regimes: from subsonic to hypersonic in continuous regime. The gas considered is a multi-species gas, thermally excited and chemically reacting. LORE is based on a finite volume formulation. Spatial discretization uses the AUSM-Van Leer scheme for inviscid flows and a centered scheme for viscous flows. The system of equations is discretized to the first order in time by linearization of the fluxes, leading to a system of algebraic equations. The algebraic system is then solved using the Gauss-Seidel relaxation method. The simulations were carried out assuming a fixed wall temperature either 300 K or 1500 K depending on the given case.

**MISTRAL** [11] is a CFD code from R-Tech solving Euler and Navier-Stokes 3D equations on a block structured mesh. The simulations of the CNES database were all carried out with the MISTRAL code. Depending on the flight point, the flow is assumed to be ideal gas flow or chemical non-equilibrium flow. In the latter case, the 5 species and 17 reactions model of Dunn & Kang is used. Finally, whatever the flight point, the wall temperature is assumed to be equal to 700 K.

The fact that the numerical database used in this study consists of mixing results from different CFD codes with different models, numerical parameters can be seen in different ways. On the one hand, there is an uncertainty associated with the numerical results obtained. This can be determined/estimated thanks to the existence of several solutions on the same case (numerical dispersion). On the other hand, the model developed from this database should be expected more robust, as it will integrate a wide range of solutions from different horizons.

#### 4. Modelling strategy and model validation

The analysis of the models described in the literature as well as the analysis of the CFD database made it possible to highlight driver parameters having a strong influence on the distribution of dimensioned heat flux: the pressure ratio  $\frac{P(x,y,z)}{P_{stag}}$ , the Mach number  $M_\infty$ , at least one geometric quantity and the object attitude  $(\alpha, \beta)$ .

The model was developed following the strategy described below:

- A first parametrization of the model was done with spherical shape;
- Followed by a wide variety of convex shape were considered;
- finally, specific developments were proposed to deal with flat surfaces.

The ratio between the local heat flux and the stagnation point heat flux calculated using the newly developed model (denoted "*New model*" in the figures) is compared with the CFD results as well as with results obtained with the Vérant-Lefrançois model (denoted "*Old model*" in the figures) for different geometric shapes: capsules, vehicles, cubes/flat plates and cylinders. For each case, the heat flux obtained with the different models was calculated using the pressure distributions from the Navier-Stokes simulations (denoted  $P_{CFD}$  in the figures) and the pressure distributions obtained using the modified Newton formula (denoted  $P_{Newton}$  in the figures).

Whatever studied case, using CFD pressure distributions or using modified Newton's pressure distributions has a very small influence on the calculated heat flux. In the case of the sphere-cone of 60° half-cone-angle in incidence of 15° (Fig. 6 and Fig. 7), the heat flux calculated using the new surrogate model makes it possible to obtain solutions very close to the numerical values both on the spherical part and the conical part, contrary to the heat flux calculated with the Vérant-Lefrançois model. On the other hand, the difference between the numerical and analytical values increases around the shoulders of the sphere-cone, inducing a significant error at this location. In the case of the '*Baseline*' shape (Fig. 8 and Fig. 9) of Hypmoces [7], the heat flux calculated by the new surrogate model is in very good agreement with the heat flux obtained by numerical simulation whether on the

convex part or the flat part of the vehicle. Finally, the results obtained on the flat plate (Fig. 10 and Fig. 11) with the new surrogate model are very close to the CFD results and allow obtaining a better prediction of the heat flux distribution than the existing models.

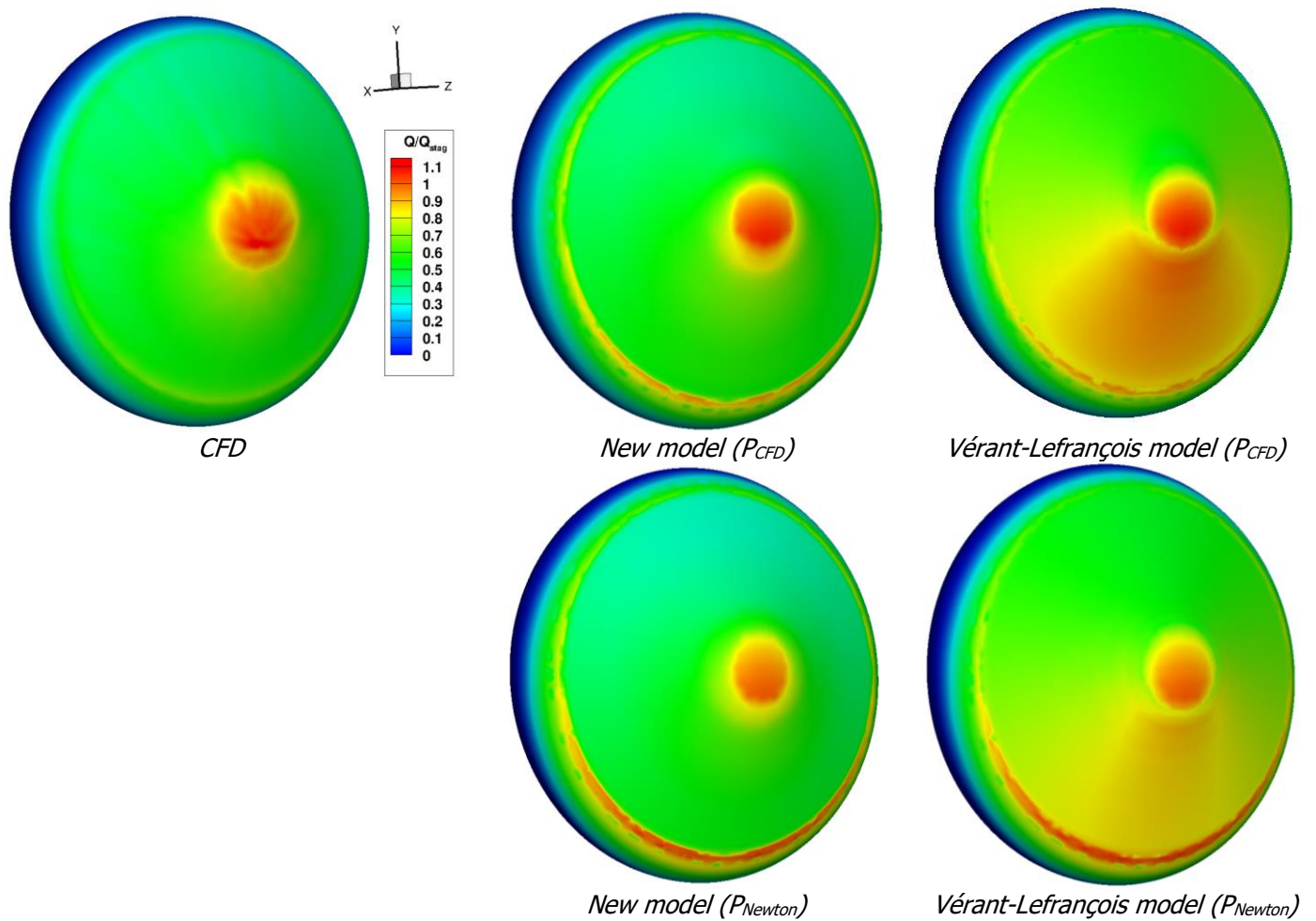


**Fig. 6.** Wall heat flux distribution for a 60° sphere-cone – Mach 22,  $\alpha = 15^\circ$ .

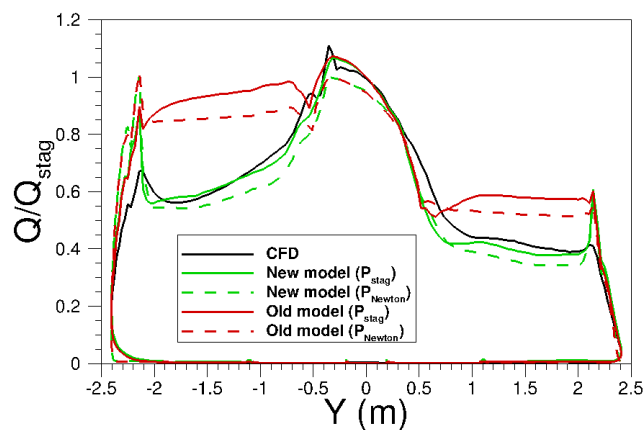


**Fig. 7.** Wall heat flux distribution along the center line of the 60° sphere-cone – Mach 22,  $\alpha = 15^\circ$ .

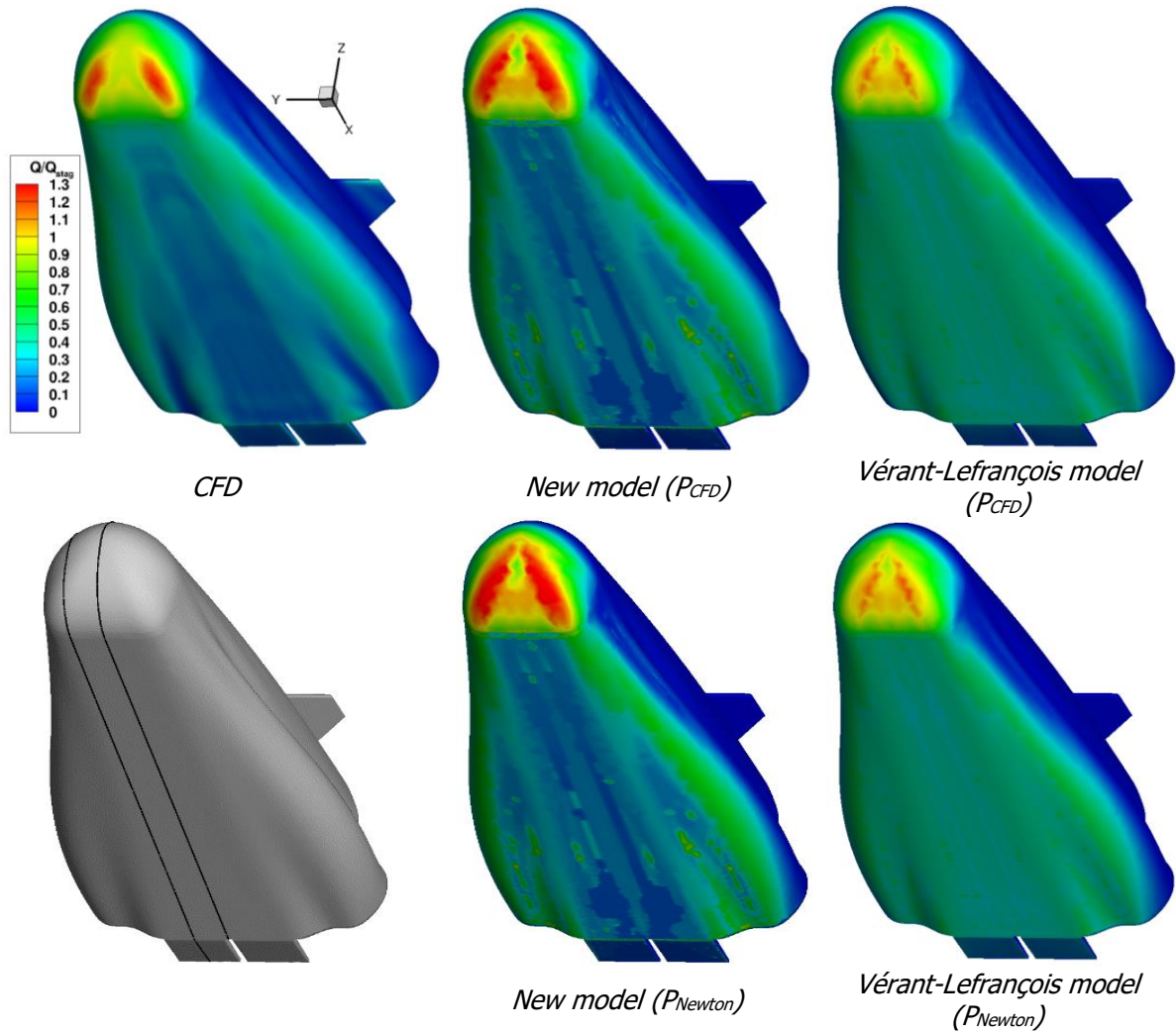


**Fig. 8.** Wall heat flux distribution at the wall of the Baseline shape of the Hypmoces vehicle – Mach 20,  $\alpha = 35^\circ$ ,  $\beta = 0^\circ$

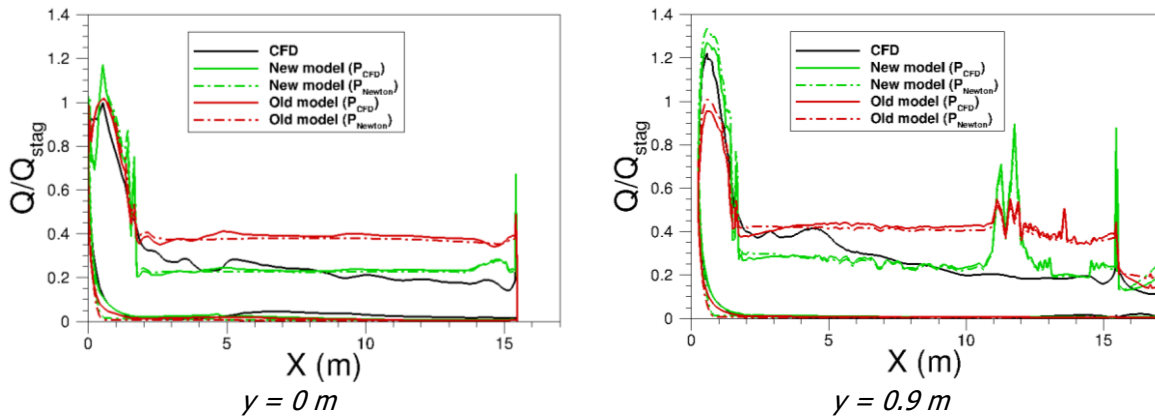


**Fig. 9.** Wall heat flux distribution along different cutting plan ( $y = 0$  m and  $y = 0.9$  m) of the Baseline shape of the Hypmoces vehicle – Mach 20,  $\alpha = 35^\circ$ ,  $\beta = 0^\circ$ .

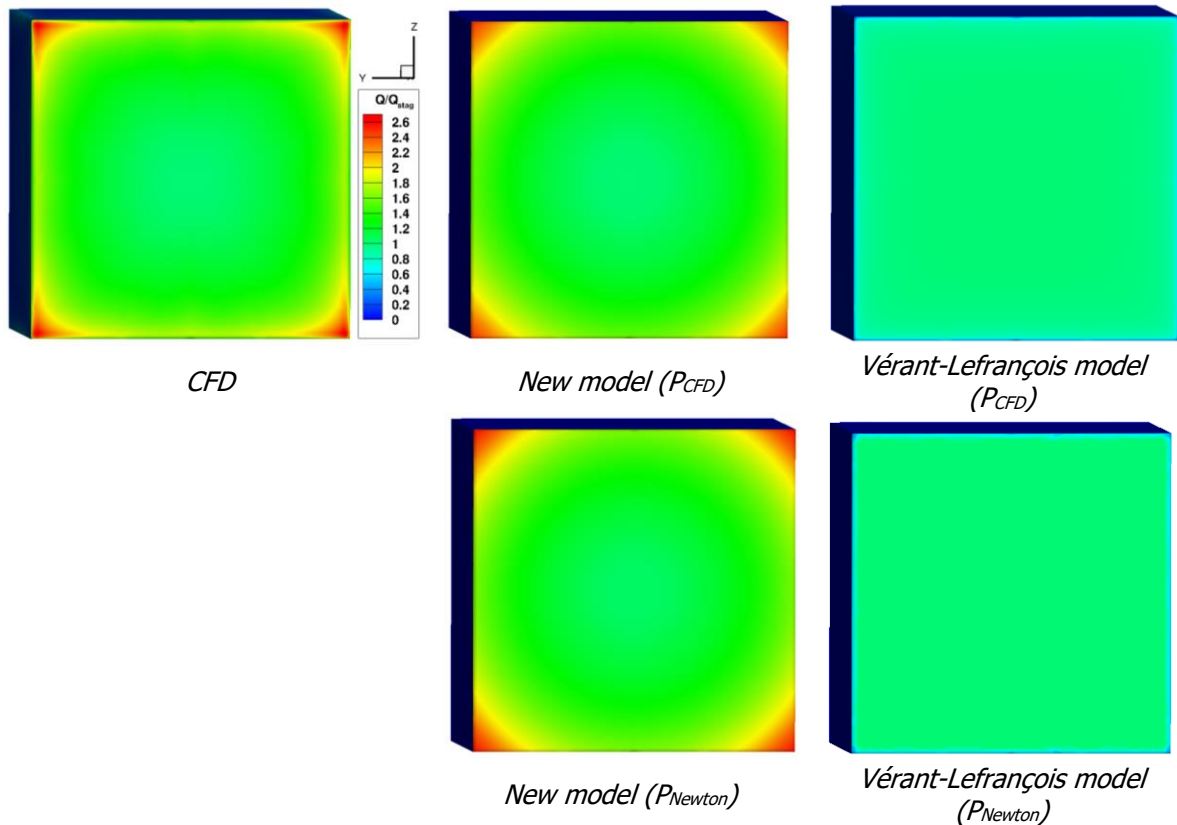


**Fig. 10.** Heat flux distribution at the wall of a 1 m cube – Mach 20,  $\alpha = 0^\circ$ .

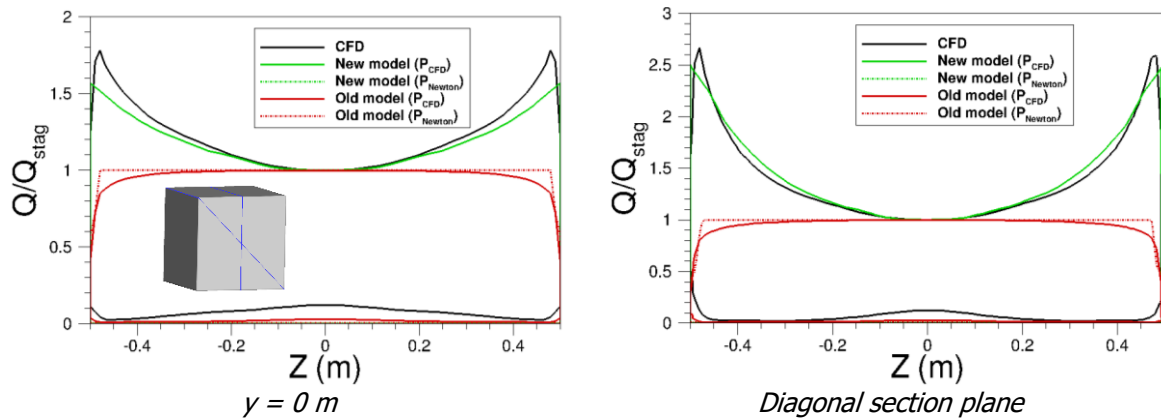


**Fig. 11.** Heat flux distribution along different cutting plan of a 1 m cube – Mach 20,  $\alpha = 0^\circ$ .

## 5. Conclusion

The literature review carried out made it possible to list existing heat flux distribution engineering models, to analyze them and to evaluate them by comparison with “high fidelity” CFD data. Then, a new heat flux distribution model was established and validated with CFD. In general, this new model provides results in good agreement with the CFD solutions on a wide variety of objects shapes and flight conditions. A significant improvement of the results is then obtained with this new surrogate model compared to those from open literature.



## Acknowledgement

This work was cofounded by ONERA (French Space Laboratory) and CNES (French Space Agency): DSO/TB/PR-2019.0018416 et DMPE/PTF-19/044-29100V1

## References

1. Lees, L.: Laminar Heat Transfer Over Blunt-Nosed Bodies at Hypersonic Flight Speeds. *J. Jet Prop.* (1959). <https://doi.org/10.2514/8.6977>
2. Kemp, N., Rose, P., Detra, R.: Laminar Heat Transfer Around Blunt Bodies in Dissociated Air. *ARS J.* (1959). <https://doi.org/10.2514/8.8128>
3. Murzinov, N. Laminar Boundary Layer on a sphere in Hypersonic Flow of Equilibrium Dissociating Air. *Fluid Dyn.* (1966). <https://doi.org/10.1007/BF01013841>
4. Prévèreaud, Y., Vérand, J-L., Balat-Pichelin, M., Moschetta, J.-M.: Numerical and experimental study of the thermal degradation process during the atmospheric re-entry of a TiAl6V4 tank. *Acta Astronautica.* (2016). <https://doi.org/10.1016/j.actaastro.2016.02.009>
5. Koppenwallner, G., Fritsche, B., Lips, T., Klinkrad, H.: SCARAB – A multi-disciplinary code for destruction analysis of Spacecraft during Re-entry. (2005). <http://adsabs.harvard.edu/pdf/2005ESASP.563..281K>
6. Merrifield, J., Beck, J., Markelov, G., Leyland, P., Molina, R.: Aerothermal Heating Methodology in the Spacecraft Aerothermal Model (SAM). In: Sgobba T., Rongier I. (eds) *Space Safety is No Accident.* Springer, Cham. (2015). [https://doi.org/10.1007/978-3-319-15982-9\\_53](https://doi.org/10.1007/978-3-319-15982-9_53)
7. Laroche, E., Prévèreaud, Y., Vérand, J-L., Sourgen, F., Bonetti, D.: Aerothermodynamics analysis of the Spaceliner Cabin Escape System modified via a morphing system. 8<sup>th</sup> European Symposium on Aerothermodynamics for Space Vehicles, Lisbon, Portugal. (2015).
8. Thivet, F., Hylkema, J., Spel, M., Dieudonné, W.: Detailed aerothermodynamical analysis of Pre-X. 4<sup>th</sup> International Symposium Atmospheric Reentry Vehicles and Systems, Arcachon, France. (2005).
9. Refloch, A., Courbet, B., Murrone, A., Villedieu, P., Laurent, C., Gilbank, P., Troyes, J., Tessé, L., Chaineray, G., Dargaud, J.B., Quémerais, E., Vuillot, F.: CEDRE Software. *Aerospace Lab. Journal.* Issue 2. (2011). <https://cedre.onera.fr/>
10. Walpot, L.: Development and application of a hypersonic flow solver. Ph.D thesis, Delft Technical University, The Netherlands. (2002).
11. Scott, T., Dieudonné, W., Spel, M.: MISTRAL - CONUS Debut Flow Field and Heat Transfer Calculations. 34<sup>th</sup> AIAA Fluid Dynamics Conference and Exhibit, Portland. (2004).